Report

Cell Reports

Pseudovirus rVSVΔG-ZEBOV-GP Infects Neurons in Retina and CNS, Causing Apoptosis and Neurodegeneration in Neonatal Mice

Graphical Abstract

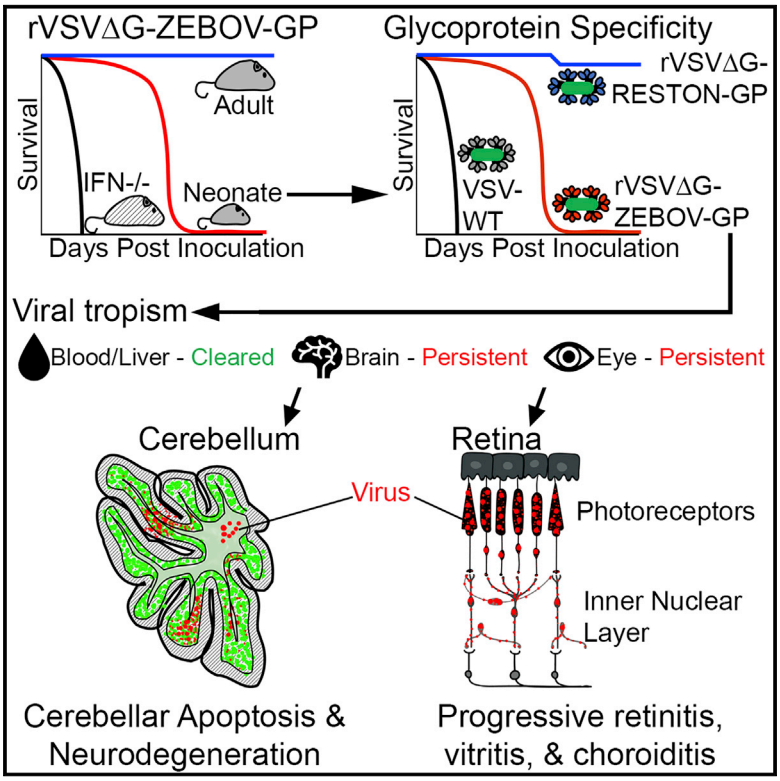

Highlights

- Replication-competent rVSVΔG-ZEBOV-GP vaccine is lethal in immunocompetent neonatal mice
- Virus is cleared from peripheral organs but persists in neurons of the eye and brain
- Mice develop severe retinitis and cerebellar apoptosis and neurodegeneration
- Co-administering poly(I:C) boosts IFN levels and protects against neurotropic infection

Authors

Ian L. McWilliams, Jennifer L. Kielczewski, Derek D.C. Ireland, ..., Rachel R. Caspi, Mohanraj Manangeeswaran, Daniela Verthelyi

Correspondence

mohanraj.manangeeswaran@fda.hhs.gov (M.M.), daniela.verthelyi@fda.hhs.gov (D.V.)

In Brief

Survivors of Ebola infections can experience neurologic and ocular symptoms, raising some concern that replication-competent vaccines expressing Ebola components could infect neurons in susceptible subjects. McWilliams et al. show that the rVSVΔG-EBOV-GP pseudovirus infects neurons in the eyes and brains of neonatal mice, causing tissue damage and lethality.

McWilliams et al., 2019, Cell Reports *26*, 1718–1726
February 12, 2019
https://doi.org/10.1016/j.celrep.2019.01.069

CellPress

OPEN ACCESS
CellPress

Cell Reports
Report

Pseudovirus rVSVΔG-ZEBOV-GP Infects Neurons in Retina and CNS, Causing Apoptosis and Neurodegeneration in Neonatal Mice

Ian L. McWilliams,[1] Jennifer L. Kielczewski,[2] Derek D.C. Ireland,[1] Jacob S. Sykes,[1] Aaron P. Lewkowicz,[1] Krishnamurthy Konduru,[3] Biying C. Xu,[2] Chi-Chao Chan,[2] Rachel R. Caspi,[2] Mohanraj Manangeeswaran,[1,*] and Daniela Verthelyi[1,4,*]

[1]Division of Biotechnology Review and Research-III, Office of Biotechnology Products, Center for Drug Evaluation and Research, Food and Drug Administration, Silver Spring, MD 20993, USA

[2]Laboratory of Immunology, National Eye Institute, NIH, Bethesda, MD 20892, USA

[3]Laboratory of Emerging Pathogens, Division of Emerging and Transfusion Transmitted Diseases, Office of Blood Research and Review, Center for Biologics Evaluation and Research, Food and Drug Administration, Silver Spring, MD 20993, USA

[4]Lead Contact

*Correspondence: mohanraj.manangeeswaran@fda.hhs.gov (M.M.), daniela.verthelyi@fda.hhs.gov (D.V.)

https://doi.org/10.1016/j.celrep.2019.01.069

SUMMARY

Zaire Ebola virus (ZEBOV) survivors experience visual and CNS sequelae that suggests the ZEBOV glycoprotein can mediate neurotropism. Replication-competent rVSVΔG-ZEBOV-GP vaccine candidate is generally well tolerated; however, its potential neurotropism requires careful study. Here, we show that a single inoculation of rVSVΔG-ZEBOV-GP virus in neonatal C57BL/6 mice results in transient viremia, neurological symptoms, high viral titers in eyes and brains, and death. rVSVΔG-ZEBOV-GP infects the inner layers of the retina, causing severe retinitis. In the cerebellum, rVSVΔG-ZEBOV-GP infects neurons in the granular and Purkinje layers, resulting in progressive foci of apoptosis and neurodegeneration. The susceptibility to infection is not due to impaired type I IFN responses, although MDA5$^{-/-}$, IFNβ$^{-/-}$, and IFNAR1$^{-/-}$ mice have accelerated mortality. However, boosting interferon levels by co-administering poly(I:C) reduces viral titers in CNS and improves survival. Although these data should not be directly extrapolated to humans, they challenge the hypothesis that VSV-based vaccines are non-neurotropic.

INTRODUCTION

Zaire Ebola virus (ZEBOV) is a highly pathogenic member of the Filoviridae family that can cause dehydration, cytokine storm, systemic bleeding, multi-organ failure, and death (Leligdowicz et al., 2016). Survivors of ZEBOV disease experience a myriad of sequelae associated with the establishment of viral reservoirs and prolonged pathology in the central nervous system (CNS) and the eyes, which suggests that the virus has neurotropic potential (Billioux et al., 2017; Howlett et al., 2018; Jacobs et al., 2016; Sagui et al., 2015; Scott et al., 2016; Varkey et al., 2015). ZEBOV glycoprotein (GP), the only viral protein on the virion surface, mediates the attachment, internalization, and endosomal release of ZEBOV into the cell, and is the prime target for most of the therapeutics and vaccines under development (González-González et al., 2017; Pavot, 2016). One vaccine under development is a live attenuated vaccine that uses a replication-competent pseudotyped vesicular stomatitis virus (VSV) platform that is being tested for multiple emergent and neglected viral diseases, including Ebola, Marburg, and Lassa viruses (Marzi et al., 2015a; World Health Organization, 2017, 2018). In this vaccine, the endogenous VSV GP was replaced with Ebola's GP (rVSVΔG-ZEBOV-GP) to confer protective immunity to Ebola and reduce the neurotropism risk of VSV (Garbutt et al., 2004).

Administration of the rVSVΔG-ZEBOV-GP virus to adult mice and non-human primates (NHPs) was generally well tolerated and generated protective immunity to the ZEBOV challenge (Garbutt et al., 2004). In clinical trials, rVSVΔG-ZEBOV-GP was tested primarily in adult subjects and children older than 6 years and shown to induce anti-GP neutralizing antibodies. Moreover, it demonstrated reasonable safety and efficacy results in ring vaccination studies in Guinea (Agnandji et al., 2017; Henao-Restrepo et al., 2017; Wong et al., 2018) and was recently redeployed to stem the 2018 outbreak in the Democratic Republic of the Congo (World Health Organization, 2000, 2018). To date, safety signals linked to the vaccine include maculopapular and vesicular dermatitis, headaches, and oligoarthritis with the presence of rVSVΔG-ZEBOV-GP in the skin lesions and synovial fluid, respectively (Agnandji et al., 2016; Huttner et al., 2015; Juan-Giner et al., 2018). It remains unclear why some subjects become symptomatic (Huttner et al., 2015), but isolation of the vaccine virus from the joints and shedding in the saliva and urine suggested that the virus can replicate to significant levels in vaccinated subjects (Agnandji et al., 2017).

Given that ZEBOV can infect and persist within the eyes and CNS of convalescent patients, there is residual concern that replacing VSV-G with the GP of ZEBOV may not eliminate the risk of neurotropism completely (Leligdowicz et al., 2016; van den Pol et al., 2017a). Preclinical studies that explored the potential

neurotropism of rVSVΔG-ZEBOV-GP in immunocompetent adult mice and NHPs did not show pseudovirus replication or CNS lesions, suggesting a lack of neurotropism (Marzi et al., 2015c; Mire et al., 2012; Suder et al., 2018) The only evidence of rVSVΔG-ZEBOV-GP entering the CNS was found in severely immunocompromised STAT1-deficient ($STAT1^{-/-}$) mice (Marzi et al., 2015b). However, in these mice, the virus spreads broadly and rapidly, killing the animals in 3–5 days, which makes this a poor model for assessing neurotropism (Marzi et al., 2015b; van den Pol et al., 2017a). Thus, with the available data, it was difficult to determine whether the documented lack of neurotropism of the rVSVΔG-ZEBOV-GP vaccine was conferred by the immune response of the host or the lack of potential neurovirulence of the vaccine.

To examine the potential neurotropism of rVSVΔG-ZEBOV-GP, we used neonatal C57BL/6 mice, which are susceptible to other RNA viruses, including Chikungunya, Zika, and Tacaribe, despite being immunocompetent (Feuer et al., 2003; Manangeeswaran et al., 2018; Pedras-Vasconcelos et al., 2006). We found that neonatal C57BL/6 mice inoculated with rVSVΔG-ZEBOV-GP developed detectable viral loads in peripheral blood and liver as early as 3 days post-inoculation (DPI). The virus was cleared from the blood and liver, but it persisted in the eyes and brains, infecting neurons and resulting in overt neurological symptoms by day 6 and death 3–9 days later. The progression of the disease depends on the innate immune response of the mice, particularly type I interferon levels, while the adaptive immune system appears dispensable. These findings highlight the potential for neurotropism of the rVSVΔG-ZEBOV-GP virus and demonstrate that the innate immune response of the host is critical to curtail its pathogenic potential.

RESULTS

rVSVΔG-ZEBOV-GP Is Lethal in Neonatal C57BL/6 Mice

As previously reported (Marzi et al., 2015b), subcutaneous (SC) inoculation with rVSVΔG-ZEBOV-GP (1,000 tissue culture infectious dose 50 [$TCID_{50}$]) is rapidly cleared and does not cause symptoms or death in adult wild-type (WT) C57BL/6 mice (Figure 1A). In contrast, the same challenge in $IFNAR1^{-/-}$resulted in 100% mortality by 3–5 DPI (Figure 1A), as previously described in adult $STAT1^{-/-}$ mice (Marzi et al., 2015b). Thus, neither model was suitable for exploring the potential neurotropism of rVSVΔG-ZEBOV-GP. Our group and others have shown that neonatal mice, while immune replete, offer a window of increased susceptibility to viral infection and are a useful model to explore viral tropism (Das and Basu, 2011; Manangeeswaran et al., 2016; Pedras-Vasconcelos et al., 2006). Therefore, we next tested the susceptibility of neonatal C57BL/6 mice to infection by inoculating 3- or 7-day-old mice (P3 or P7, respectively) with 1,000 $TCID_{50}$ rVSVΔG-ZEBOV-GP SC. P7 mice inoculated with the vaccine virus showed transient mild tremors, but they recovered and had 100% survival (Figure 1A). In contrast, P3 mice developed signs of severe neurological disease that started with tremors, widened stance, and ataxia and progressed to seizures and paresis and/or paralysis; they succumbed to disease by 15 DPI (Figure 1A).

To determine whether the disease caused by rVSVΔG-ZEBOV-GP was driven by the GP, we compared their disease progression with that of mice that received similar inoculums of the parental VSV (Indiana strain), rVSVΔG-ZEBOV-GPΔMUCIN, a VSV pseudovirus that expresses the ZEBOV GP with a deleted mucin domain, or rVSVΔG-RESTON-GP, in which the G of VSV is replaced by the Reston Ebola GP (Lee et al., 2017). P3 mice inoculated with the parental VSV strain succumbed 3–5 days post-challenge, whereas mice inoculated with rVSVΔG-RESTON-GP showed a weight gain similar to uninfected mice and survived the challenge (Figure 1B). Mice inoculated with rVSVΔG-ZEBOV-GP and those that received rVSVΔG-ZEBOV-GPΔMUCIN showed a similar disease progression, suggesting that the mucin domain of ZEBOV GP does not play a critical role in this model. Although at this time we do not know why mice infected with rVSVΔG-RESTON-GP survive the challenge, the data suggest that the GP expressed by the VSV pseudovirus is a key determinant of the rate of infection and pathology in these mice, as previously suggested (van den Pol et al., 2017a).

Next, we examined whether the susceptibility of P3 mice to infection was associated with a reduced ability to mount an interferon response by comparing their *in vivo* response to poly(I:C) (50 μg/mouse, SC) inoculation with that of P7 mice, which are resistant to the challenge. P3 and P7 mice showed similar levels of mRNA for interferon (IFN)-stimulated genes (ISGs) *ccl5*, *cxcl10*, *irf7*, and *isg15* in peripheral blood 24 h post-treatment (Figure 1C), suggesting that the lethal neurotropic infection induced by rVSVΔG-ZEBOV-GP vaccine was not due to an intrinsic IFN deficiency in neonatal mice.

Since P3 infected mice developed symptoms that are consistent with neurotropic infection, we confirmed the involvement of the CNS following rVSVΔG-ZEBOV-GP vaccination. Quantification of viral titer at 3 DPI (pre-symptomatic time point), 6 DPI (symptomatic time point), and 9 DPI (pre-morbidity time point) in peripheral blood, livers, eyes, and brains by $TCID_{50}$ analysis showed a transient infection in the blood and liver, peaking at 6 DPI and ultimately resolving by 9 DPI (Figure 1D). In contrast, there were sustained high levels of virus in brains and eyes (Figure 1D). This showed that the mice can effectively clear rVSVΔG-ZEBOV-GP from peripheral organs but not from the brain or the eye, which is consistent with the reports of persistent ocular and neurological involvement in patients infected with Ebola (Eligdowicz et al., 2016; Varkey et al., 2015).

rVSVΔG-ZEBOV-GP Infects Neuronal Cells of the Retina in Neonatal Mice

Having established that the virus infects the eyes of vaccinated mice, we next assessed whether the infection was associated with pathologic changes in the tissue. Histological examination confirmed that the infection causes progressive retinitis, vitritis, and choroiditis, with cellular infiltration and retinal edema (Figure 2A). Staining with anti-GP-specific antibody KZ52 at 3, 6, and 9 DPI showed a gradual increase in viral antigen that is associated with progressive disorganization of the retinal layers in the eye as compared to non-infected controls (Figure 2B). The morphology and localization of the infected cells suggest that amacrine, horizontal, and bipolar cells are infected with

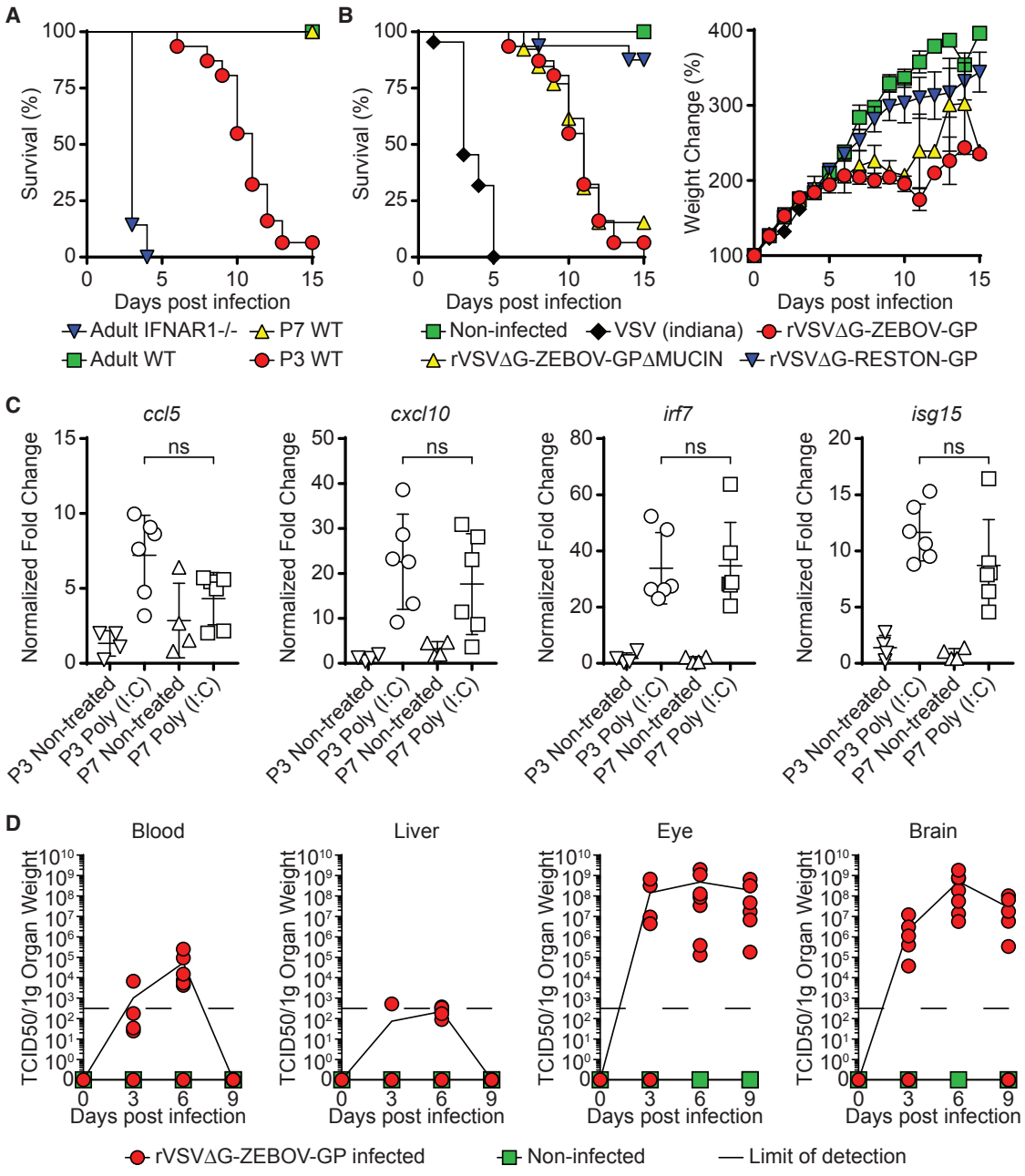

Figure 1. Inoculation of rVSVΔG-ZEBOV-GP Causes Lethal Infection with Eye and Brain Involvement in Neonatal C57BL/6 Mice

(A) Adult IFNAR1$^{-/-}$ (inverted blue triangles, n = 7), adult WT (green squares, n = 7), P7 WT (yellow triangles, n = 8), and WT P3 (red circles, n = 31) mice were challenged with 1,000 $TCID_{50}$ of rVSVΔG-ZEBOV-GP and monitored for survival.

(B) P3 WT mice were challenged with saline (non-infected, green squares, n = 8), VSV (Indiana strain, black diamonds, n = 22), rVSVΔG-ZEBOV-GPΔMUCIN (yellow triangles, n = 13), or rVSVΔG-RESTON-GP (inverted blue triangles, n = 16) and monitored for survival and weight change (data shown as means ± SEMs). P3 rVSVΔG-ZEBOV-GP infection survival and weight change is shown for comparison (red circles). Note that P3 mice that received rVSVΔG-RESTON-GP survived the length of the study (3 months).

(C) P3 and P7 mice were treated with poly(I:C) (50 μg/mouse). Expression of *ccl5*, *cxcl10*, *irf7*, and *isg15* in peripheral blood was measured after 24 h. Data shown as means ± SDs. Statistical differences were tested using an unpaired two-tailed t test (ns, not statistically significant).

(D) Quantification of virus levels using $TCID_{50}$ analysis was performed in non-infected and rVSVΔG-ZEBOV-GP-infected mice at 3, 6, and 9 DPI (n = 7/group) in the blood, liver, eye, and brain. Data represent means ± SDs. Data represent 2–5 independent experiments.

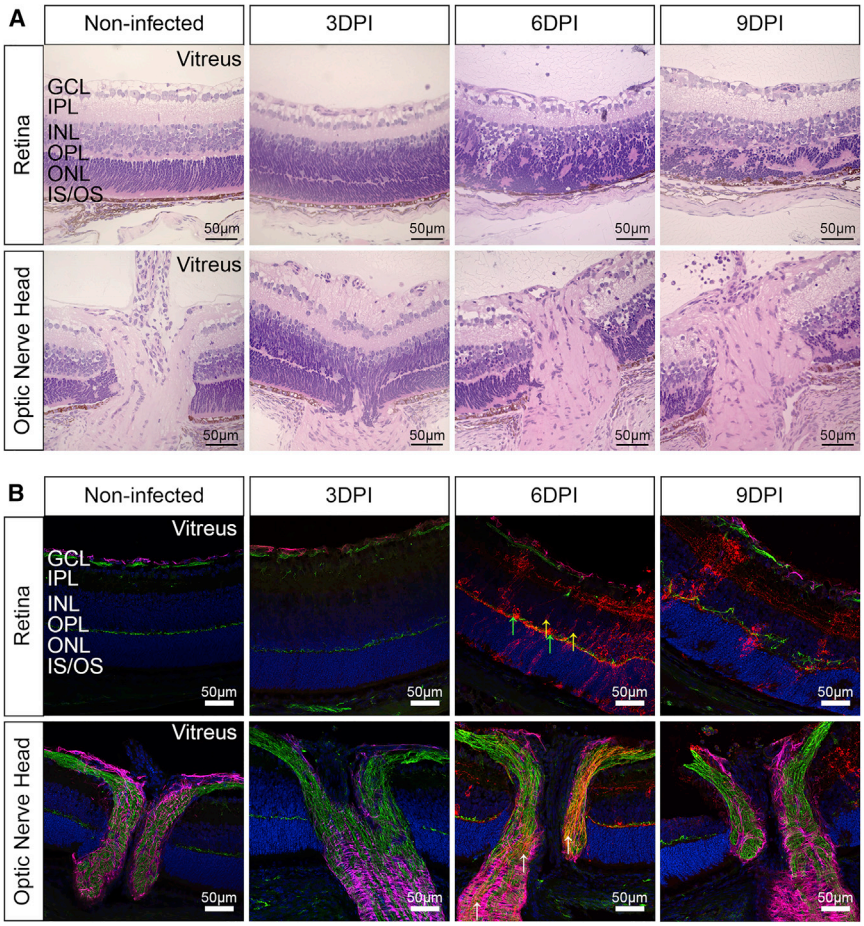

Figure 2. rVSVΔG-ZEBOV-GP Infects the Retina and Optic Nerve Head

Non-infected and rVSVΔG-ZEBOV-GP-infected eyes were collected at 3, 6, and 9 DPI.

(A) Sections of the eye were stained with H&E to assess pathology. Scale bars, 50 μm.

(B) Eye sections (retina and optic nerve head) were stained with antibodies to ZEBOV GP (red), GFAP (magenta), neurofilament (green), or DAPI (blue). Yellow arrows indicate bipolar cells; green arrows indicate horizontal cells; and white arrows denote virus within the optic nerve. Data represent 2 independent experiments, with n = 6 (non-infected) and n = 12 (infected) mice per group. Scale bars, 50 μm.

substantial loss of their cell body, axons, and dendrites, resulting in the thinning of the inner nuclear layer (INL), the inner plexiform layer (IPL), and the outer plexiform layer (OPL), with clear damage to the outer nuclear layer (ONL) and photoreceptor layer by 9 DPI. This shows that rVSVΔG-ZEBOV-GP can infect the eye, leading to cellular infiltration and severe disruption of the retinal architecture.

rVSVΔG-ZEBOV-GP Infects Neurons and Purkinje Cells of the Midbrain and Cerebellum

Immunohistochemical (IHC) analysis of the CNS at 3, 6, and 9 DPI using antibodies to ZEBOV GP and NeuN showed that early on, the virus infects predominantly the midbrain and the posterior brain (Figure 3A). Specifically, viral antigen can be detected in the midbrain, as well as in the white matter tracks and deep nuclei of the cerebellum by 3 DPI compared to uninfected controls. At 6 DPI, there are large foci of virus in the molecular layer of the cerebellum. By 9 DPI, there is no evidence of virus in the midbrain, but the cerebellum shows extensive areas stained with viral antigen, predominantly in the granular and Purkinje layers, and disruption of the cerebellar architecture.

To better understand viral tropism, we performed confocal microscopy on sections of cerebellum at 6 DPI, before the tissue became disorganized. Staining for ZEBOV GP, neurofilament heavy chain (anti-SMI-31 and SMI-32), Purkinje cells (Gad67), or astrocytes (glial fibrillary acidic protein [GFAP]) shows that viral antigen co-localizes with neurofilament, particularly in the granular layer of cerebellum, indicating that neurons are predominantly infected (Figure 3B). Purkinje and granule cells, as well as possibly stellate and basket cells, appear to be susceptible to infection (Figure 3B). Orthogonal analysis of the confocal images confirmed the co-localization of Gad67 and neurofilament with viral antigen (Figure S1A). In contrast, there was no co-localization of viral antigen with GFAP (Figures S1B and S1C), indicating that astrocytes are not infected. These data demonstrate that rVSVΔG-ZEBOV-GP infects the CNS, is cleared from most of the cerebrum, but persists in cerebellum, where it primarily infects neurons.

The disruption of cerebellar architecture in areas rich in viral antigen suggested that the infection led to local tissue damage; therefore, TUNEL and Fluoro-Jade C staining was used to assess apoptosis or neurodegeneration, respectively. Brain sections taken at 9 DPI and stained for TUNEL, NeuN, and ZEBOV GP show extensive apoptosis, particularly in the $NeuN^+$-rich granular layer of the cerebellum (Figure 3C) and not the $GFAP^+$ regions (Figure S2). Similarly, Fluoro-Jade C staining indicates foci of neurodegeneration in the cerebellum in the areas corresponding to those with high levels of viral antigen (Figure 3D). These data indicate that following inoculation, rVSVΔG-ZEBOV-GP infects the CNS of neonatal mice, localizing predominantly to granular and Purkinje layers of the cerebellum, resulting in apoptosis and neurodegeneration, which are consistent with the ataxia observed in the mice.

Innate Immune Response Modulates Susceptibility to Viral Infection

The mechanism underlying the increased susceptibility of neonatal mice to infection remains unclear. To determine

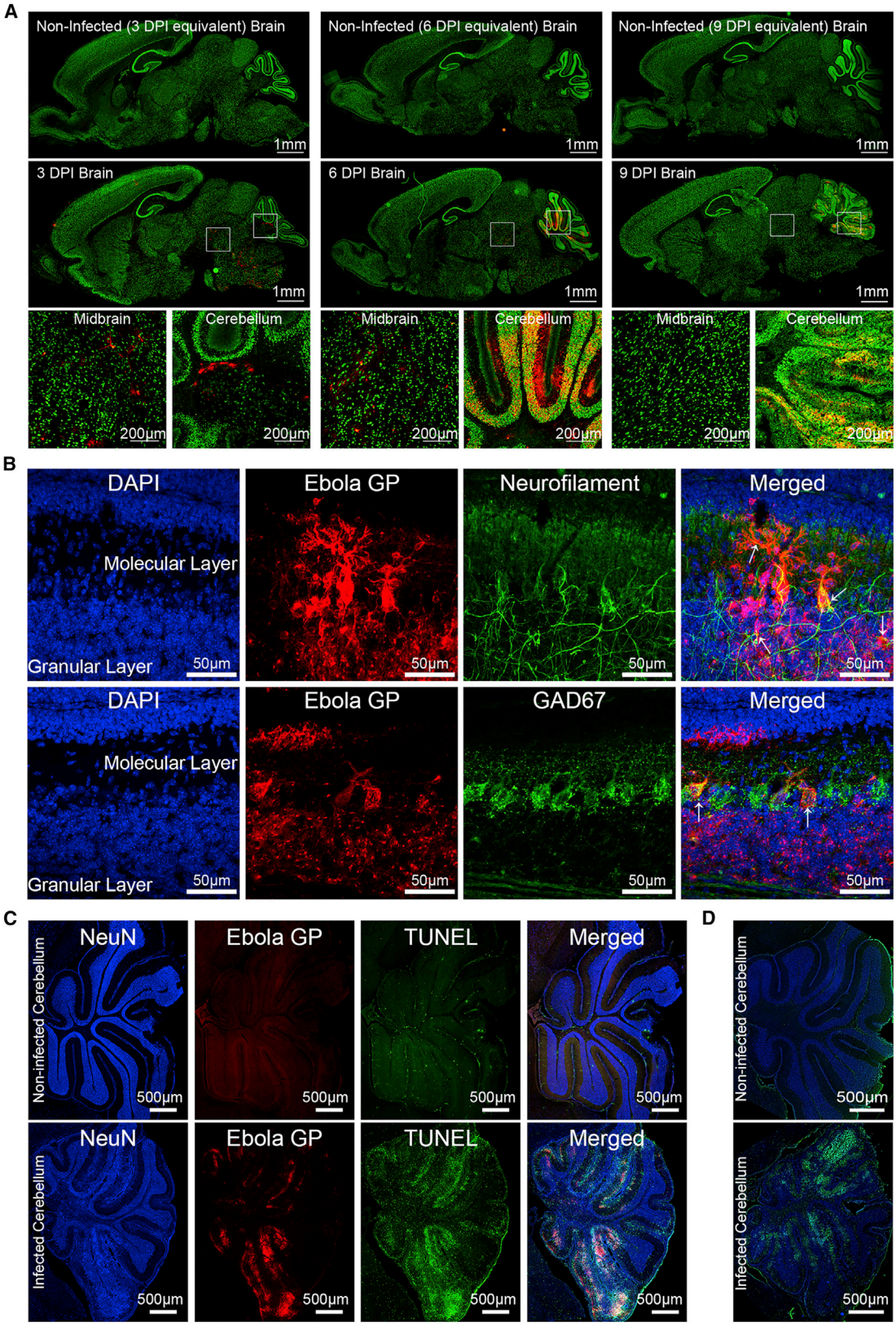

(legend on next page)

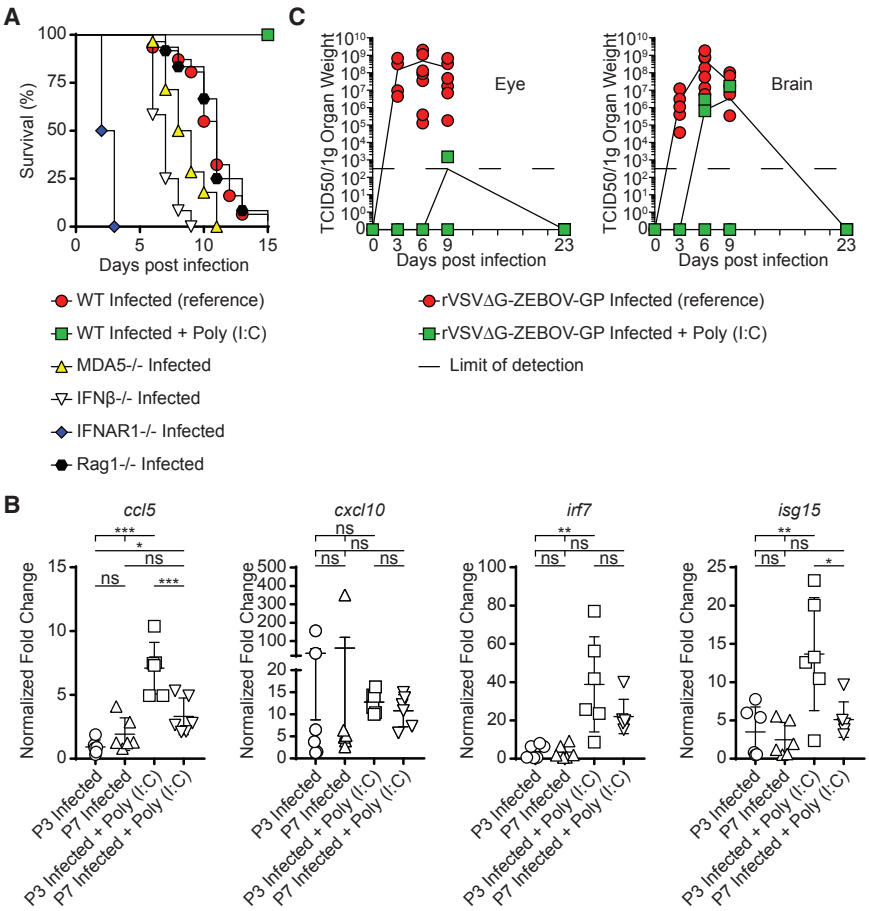

Figure 4. Interferon Responses Affect Susceptibility to rVSVΔG-ZEBOV-GP Infection

(A) Disease progression in P3 C57BL/6 mice (red circles) challenged with rVSVΔG-ZEBOV-GP virus was compared with age-matched innate immunodeficient IFNAR1$^{-/-}$ (blue diamonds, n = 12), IFNβ$^{-/-}$ (empty inverted triangles, n = 12), and MDA5$^{-/-}$ (yellow triangles, n = 28) mice, as well as adaptive immunodeficient RAG1$^{-/-}$ mice (black hexagons, n = 12). Infected P3 C57BL/6 mice were co-treated with poly(I:C) (50 μg, green squares, n = 8).

(B) Gene expression of *ccl5*, *cxcl10*, *irf7*, and *isg15* was measured in the peripheral blood of P3 and P7 neonatal mice inoculated with rVSVΔG-ZEBOV-GP ± poly(I:C) co-treatment. Data shown as means ± SDs. Statistical differences were tested using one-way ANOVA with post hoc Tukey's multiple comparison test (ns, not statistically significant; *p < 0.05, **p < 0.01, and ***p < 0.001).

(C) P3 C57BL/6 mice inoculated with rVSVΔG-ZEBOV-GP alone (red) or together with 50 μg poly(I:C) (green). Viral loads in the eye and brain were determined by $TCID_{50}$ at 3 (n = 5), 6 (n = 5), 9 (n = 5), and 23 DPI (n = 8). Data represent 2–5 independent experiments.

whether an immature adaptive immune system would contribute to the susceptibility to infection in neonatal mice, we inoculated P3 RAG1$^{-/-}$ mice lacking B and T cells. These mice showed a survival curve similar to that of WT C57BL/6 mice, suggesting that T and B lymphocytes neither protect neonatal mice from a challenge with rVSVΔG-ZEBOV-GP nor modify the disease progression (Figure 4A). Type I IFNs are known to play a critical role in resisting viral infections. Although P3 mice developed a lethal disease following rVSVΔG-ZEBOV-GP inoculation, while P7 mice were resistant, P3 and P7 mice showed a similar increase in the expression of ISGs *ccl5*, *cxcl10*, *irf7*, and *isg15* 24 h post-challenge (Figure 4B). Moreover, infected P3 mice retained their ability to mount an IFN response upon stimulation with poly(I:C), as demonstrated by the increased expression for several ISGs (Figure 4B), which is comparable to that of uninfected P3 or P7 mice (Figure 1C). Despite this, the progression of the disease appeared to be linked to the type I IFN responses—P3 IFNAR1$^{-/-}$ mice succumbed 2–3 DPI and P3 IFNβ$^{-/-}$ and MDA5$^{-/-}$ mice, which have a partial defect in their type I IFN responses, succumbed 6–8 DPI (Figure 4A). Thus, mice with reduced IFN responses showed accelerated death as compared to C57BL/6 or RAG1$^{-/-}$, which have intact IFN responses (Figure 4A). This suggests that the susceptibility to infection in neonates is not mediated by a defect in IFN responses, but the levels of IFNs' affect disease progression. To confirm this, we explored whether increasing the IFN levels would prolong survival. Administration of poly(I:C) at the time of inoculation with rVSVΔG-ZEBOV-GP did not preclude mice from becoming infected, since the virus was detectable in the brain and eye (Figure 4C), but resulted in lower virus titers and 100% survival (Figure 4A). This suggests that ensuring a strong IFN response at the time of inoculation may enhance the immune

Figure 3. Neurotropic rVSVΔG-ZEBOV-GP Infection in the Brain

C57BL/6 mice (P3) were inoculated with rVSVΔG-ZEBOV-GP, and brains were collected for IHC at 3, 6, and 9 DPI.

(A) Sagittal sections of non-infected (n = 7) and infected (n = 9) mice were stained with antibodies to Ebola GP (red) and NeuN (green); scale bars, 1 mm. Boxed areas of infected midbrain and cerebellum regions are shown below; scale bars, 200 μm.

(B) Confocal microscopy was performed on 6 DPI brain sections (n = 3) stained with DAPI (blue), Ebola GP (red), and either neurofilament (green) or GAD67 (green); scale bars, 50 μm. Right: merged images (red + blue + green). White arrows indicate infected cells.

(C) Non-infected (n = 4) and rVSVΔG-ZEBOV-GP-infected (n = 5) sections were stained with antibodies to NeuN (blue), apoptosis marker TUNEL (green), and ZEBOV GP (red) at 9 DPI. Right: merged images. Scale bars, 500 μm.

(D) Non-infected (n = 4) and rVSVΔG-ZEBOV-GP-infected (n = 9) sections were stained with Fluoro-Jade C (green), a marker for neurodegeneration, and DAPI (blue); scale bars, 500 μm. Data represent 2–4 independent experiments.

response to the virus and reduce the risk of dissemination to the CNS.

DISCUSSION

The broad tissue tropism and low levels of preexisting immunity make VSV an appealing platform for vaccine development for emerging and reemerging infectious diseases, including Ebola, Marburg, influenza, and Nipah (van den Pol et al., 2017a). Presently, this strategy involves replacing the VSV-G with the viral GP of interest. These vaccines differ from previous live virus vaccines, such as the yellow fever vaccine, which were attenuated either by multiple passages in cell culture or by targeted genetic mutations, in that for VSV-based vaccines, the attenuation is based solely on the replacement of the VSV G. While these chimeric viruses have demonstrated a good safety profile in animal models, some data suggest that some constructs could be neurotropic and pathogenic (van den Pol et al., 2017a). For Ebola, previous preclinical studies in adult mice and NHPs suggested that the vaccine does not replicate in the CNS, even when injected intrathecally (Mire et al., 2012). However, recent studies show that 60% of survivors of the 2014–2016 ZEBOV disease outbreak present with ocular symptoms, including uveitis, retinitis, and cataracts (Mattia et al., 2016; Steptoe et al., 2017). Furthermore, there are reports of neurological and psychiatric disease and even detectable virus in the cerebrospinal fluid of convalescent patients (Billioux et al., 2017; Jacobs et al., 2016; Sagui et al., 2015). These data suggest that the GP of Ebola can mediate neurotropism in the right clinical context and that some animal models, including NHPs, may fail to fully recapitulate human disease.

The mechanisms underlying the increased susceptibility to neurotropism in young mice are unknown but may be rooted in the high frequency of mitotically active immature neurons and neuronal precursors, active pruning, and differential expression pattern of cellular receptors, which may be used by the virus to gain entry (Feuer et al., 2005; Miner and Diamond, 2016). Alternatively, mildly impaired immune responses to the virus can result in unchecked virus proliferation (Lee and Ashkar, 2018). In our study, P3 and P7 C57BL/6 mice displayed similar ISG responses when challenged with virus or poly(I:C), and infection did not modify the response to poly(I:C). Furthermore, P3 mice responded to treatment with poly(I:C) by mounting an effective response that improves survival. Thus, it seems likely that the increased susceptibility of neonatal mice is not linked to a defective IFN response. Moreover, adult RAG1$^{-/-}$ mice, which lack mature T and B cells but have intact IFN responses, were not susceptible to infection, while neonatal RAG1$^{-/-}$ mice had disease kinetics upon inoculation similar to those of WT mice, suggesting that the adaptive immune response does not contribute to susceptibility to infection. These results are consistent with previous reports showing that simian immunodeficiency virus (SIV)-infected NHPs with greatly reduced CD4 T cell counts control rVSVΔG-ZEBOV-GP infection, as do healthy NHPs (Geisbert et al., 2008). These data suggest that the increased susceptibility of neonatal mice to neurotropic infection with rVSVΔG-ZEBOV-GP may be developmental, rather than linked to defects in the neonatal immune system, as previously reported for other viruses such as measles, Zika, and Sindbis virus (Ganesan et al., 2018; van den Pol et al., 2017b; Vernon and Griffin, 2005). The mechanisms underlying susceptibility in neonatal mice may be different from those underlying CNS or eye infections in patients with EBOV. Future studies will need to address the exact determinants that confer susceptibility to infection, as this may help researchers to understand what populations may be more vulnerable to the vaccine and identify the determinants of susceptibility to eye and CNS sequelae in patients infected with ZEBOV.

As noted above, ZEBOV can cause neurological and ocular symptoms in children and adult patients, suggesting that neurotropism in humans may be less restricted than in mice. The lesions observed in the cerebellums of the challenged neonatal mice are reminiscent of the reports of cerebellar atrophy and strokes reported in Ebola survivors (Howlett et al., 2018). Similarly, the severe retinopathies that developed in the neonatal mice recall the uveitis, retinitis, and cataracts described in many of the 2014 survivors (Mattia et al., 2016; Steptoe et al., 2017). This suggests that the neonatal C57BL/6 model may be more representative of the viral tropism in humans than that of IFNAR1$^{-/-}$ and STAT1$^{-/-}$ mice, which succumb to infection within 5 days of inoculation (Marzi et al., 2015b). Nonetheless, as with any animal model, these results must be considered carefully as there are extensive clinical data from healthy adults and older children indicating that the present vaccine is generally safe, although there could be an increased risk to pregnant women and other vulnerable populations (Heppner et al., 2017; Juan-Giner et al., 2018; Lennemann et al., 2017).

Lastly, our study shows that co-administering poly(I:C) at the time of inoculation may enhance viral clearance and reduce the risk of neurotropism. Of note, treatment with poly(I:C) did not modify the disease course of IFNAR1$^{-/-}$ mice (Figure S3), indicating that the protective effect required a type I IFN response. This suggests that Toll-like receptor 3 (TLR3), TLR9, or TLR7 agonists could be harnessed to improve the safety of the vaccine in at-risk or susceptible populations.

In summary, our results suggest that the apparent safety of the vaccine and absence of neurological signals is likely dependent on the neurodevelopmental and immune status of the host rather than the absence of the neurotropic potential of the virus. Although these data cannot be directly extrapolated to humans, they challenge the notion that VSV-based vaccines are non-neurotropic when the endogenous G is replaced with a different viral GP (Marzi et al., 2015b; Rose et al., 2000). Carefully designed clinical studies may help to establish the safety of vaccinations using this platform in potentially highly susceptible populations such as pregnant mothers and infants. Further studies may determine whether the addition of innate immunomodulators could reduce the potential risk of neurotropism in a susceptible population while maintaining the protective effect of the vaccines.

STAR★METHODS

Detailed methods are provided in the online version of this paper and include the following:

- KEY RESOURCES TABLE
- CONTACT FOR REAGENT AND RESOURCE SHARING

SUPPLEMENTAL INFORMATION

Supplemental Information includes three figures and can be found with this article online at https://doi.org/10.1016/j.celrep.2019.01.069.

ACKNOWLEDGMENTS

The assertions herein are private ones from the authors and are not to be construed as official or reflecting the views of the US Food and Drug Administration. The authors wish to thank Jill Ascher, Mary Belcher, and the personnel of the animal facility for the care of the mice. We thank Steven Rubin, Dino Feigelstock, and Amy Rosenberg for useful discussions and reviewing the manuscript; Gerardo Kaplan for the rVSVΔG-ZEBOV-GPΔMUCIN virus; Keith Peden for the rVSVΔG-RESTON-GP virus; and Maiu Romano-Verthelyi for help with the graphical abstract. This study was supported in part by Senior Postgraduate Research Fellowship Awards to I.L.M., A.P.L., and J.S.S. from the Oak Ridge Institute for Science and Education through an interagency agreement between the US Department of Energy and the US Food and Drug Administration. Lastly, this work was partly supported by grants funded by the FDA's Office of Counter-terrorism and Emergency Coordination.

AUTHOR CONTRIBUTIONS

I.L.M., M.M., and D.V. conceived this study and drafted the manuscript. I.L.M. performed the data analysis and all *ex vivo* and *in vivo* experiments. D.D.C.I., J.S.S., and A.P.L. performed the brain ICC and confocal imaging. J.L.K. performed the eye ICC, and B.C.X. facilitated the eye immunohistochemistry (IHC). C.-C.C. and R.R.C. contributed their analysis and expertise in the eye data. K.K. developed the rVSVΔG-ZEBOV-GPΔMUCIN construct.

DECLARATION OF INTERESTS

The authors declare no competing interests.

Received: July 3, 2018
Revised: November 15, 2018
Accepted: January 17, 2019
Published: February 12, 2019

REFERENCES

Agnandji, S.T., Huttner, A., Zinser, M.E., Njuguna, P., Dahlke, C., Fernandes, J.F., Yerly, S., Dayer, J.A., Kraehling, V., Kasonta, R., et al. (2016). Phase 1 Trials of rVSV Ebola Vaccine in Africa and Europe. N. Engl. J. Med. *374*, 1647–1660.

Agnandji, S.T., Fernandes, J.F., Bache, E.B., Obiang Mba, R.M., Brosnahan, J.S., Kabwende, L., Pitzinger, P., Staarink, P., Massinga-Loembe, M., Krähling, V., et al.; VEBCON Consortium (2017). Safety and immunogenicity of rVSVΔG-ZEBOV-GP Ebola vaccine in adults and children in Lambaréné, Gabon: a phase I randomised trial. PLoS Med. *14*, e1002402.

Billioux, B.J., Nath, A., Stavale, E.J., Dorbor, J., Fallah, M.P., Sneller, M.C., and Smith, B.R.; Partnership for Research on Ebola Virus in Liberia (PREVAIL) III Study Group (2017). Cerebrospinal fluid examination in survivors of ebola virus disease. JAMA Neurol. *74*, 1141–1143.

Das, S., and Basu, A. (2011). Viral infection and neural stem/progenitor cell's fate: implications in brain development and neurological disorders. Neurochem. Int. *59*, 357–366.

Feuer, R., Mena, I., Pagarigan, R.R., Harkins, S., Hassett, D.E., and Whitton, J.L. (2003). Coxsackievirus B3 and the neonatal CNS: the roles of stem cells, developing neurons, and apoptosis in infection, viral dissemination, and disease. Am. J. Pathol. *163*, 1379–1393.

Feuer, R., Pagarigan, R.R., Harkins, S., Liu, F., Hunziker, I.P., and Whitton, J.L. (2005). Coxsackievirus targets proliferating neuronal progenitor cells in the neonatal CNS. J. Neurosci. *25*, 2434–2444.

Ganesan, P., Chandwani, M.N., Creisher, P.S., Bohn, L., and O'Donnell, L.A. (2018). The neonatal anti-viral response fails to control measles virus spread in neurons despite interferon-gamma expression and a Th1-like cytokine profile. J. Neuroimmunol. *316*, 80–97.

Garbutt, M., Liebscher, R., Wahl-Jensen, V., Jones, S., Möller, P., Wagner, R., Volchkov, V., Klenk, H.D., Feldmann, H., and Ströher, U. (2004). Properties of replication-competent vesicular stomatitis virus vectors expressing glycoproteins of filoviruses and arenaviruses. J. Virol. *78*, 5458–5465.

Geisbert, T.W., Daddario-Dicaprio, K.M., Lewis, M.G., Geisbert, J.B., Grolla, A., Leung, A., Paragas, J., Matthias, L., Smith, M.A., Jones, S.M., et al. (2008). Vesicular stomatitis virus-based ebola vaccine is well-tolerated and protects immunocompromised nonhuman primates. PLoS Pathog. *4*, e1000225.

González-González, E., Alvarez, M.M., Márquez-Ipiña, A.R., Trujillo-de Santiago, G., Rodríguez-Martínez, L.M., Annabi, N., and Khademhosseini, A. (2017). Anti-Ebola therapies based on monoclonal antibodies: current state and challenges ahead. Crit. Rev. Biotechnol. *37*, 53–68.

Henao-Restrepo, A.M., Camacho, A., Longini, I.M., Watson, C.H., Edmunds, W.J., Egger, M., Carroll, M.W., Dean, N.E., Diatta, I., Doumbia, M., et al. (2017). Efficacy and effectiveness of an rVSV-vectored vaccine in preventing Ebola virus disease: final results from the Guinea ring vaccination, open-label, cluster-randomised trial (Ebola Ça Suffit!). Lancet *389*, 505–518.

Heppner, D.G., Jr., Kemp, T.L., Martin, B.K., Ramsey, W.J., Nichols, R., Dasen, E.J., Link, C.J., Das, R., Xu, Z.J., Sheldon, E.A., et al.; V920-004 Study Team (2017). Safety and immunogenicity of the rVSVΔG-ZEBOV-GP Ebola virus vaccine candidate in healthy adults: a phase 1b randomised, multicentre, double-blind, placebo-controlled, dose-response study. Lancet Infect. Dis. *17*, 854–866.

Howlett, P.J., Walder, A.R., Lisk, D.R., Fitzgerald, F., Sevalie, S., Lado, M., N'jai, A., Brown, C.S., Sahr, F., Sesay, F., et al. (2018). Case Series of Severe Neurologic Sequelae of Ebola Virus Disease during Epidemic, Sierra Leone. Emerg. Infect. Dis. *24*, 1412–1421.

Huttner, A., Dayer, J.A., Yerly, S., Combescure, C., Auderset, F., Desmeules, J., Eickmann, M., Finckh, A., Goncalves, A.R., Hooper, J.W., et al.; VSV-Ebola Consortium (2015). The effect of dose on the safety and immunogenicity of the VSV Ebola candidate vaccine: a randomised double-blind, placebo-controlled phase 1/2 trial. Lancet Infect. Dis. *15*, 1156–1166.

Jacobs, M., Rodger, A., Bell, D.J., Bhagani, S., Cropley, I., Filipe, A., Gifford, R.J., Hopkins, S., Hughes, J., Jabeen, F., et al. (2016). Late Ebola virus relapse causing meningoencephalitis: a case report. Lancet *388*, 498–503.

Juan-Giner, A., Tchaton, M., Jemmy, J.P., Soumah, A., Boum, Y., Faga, E.M., Cisse, M., and Grais, R.F. (2018). Safety of the rVSV ZEBOV vaccine against Ebola Zaire among frontline workers in Guinea. Vaccine, S0264-410X(18)31246-5.

Lee, A.J., and Ashkar, A.A. (2018). The Dual Nature of Type I and Type II Interferons. Front. Immunol. *9*, 2061.

Lee, S.S., Phy, K., Peden, K., and Sheng-Fowler, L. (2017). Development of a micro-neutralization assay for ebolaviruses using a replication-competent vesicular stomatitis hybrid virus and a quantitative PCR readout. Vaccine *35*, 5481–5486.

Leligdowicz, A., Fischer, W.A., 2nd, Uyeki, T.M., Fletcher, T.E., Adhikari, N.K., Portella, G., Lamontagne, F., Clement, C., Jacob, S.T., Rubinson, L., et al. (2016). Ebola virus disease and critical illness. Crit. Care *20*, 217.

Lennemann, N.J., Herbert, A.S., Brouillette, R., Rhein, B., Bakken, R.A., Perschbacher, K.J., Cooney, A.L., Miller-Hunt, C.L., Ten Eyck, P., Biggins, J., et al. (2017). Vesicular stomatitis virus pseudotyped with Ebola virus glycoprotein serves as a protective, non-infectious vaccine against Ebola virus challenge in mice. J. Virol., JVI.00479-17.

Manangeeswaran, M., Ireland, D.D.C., and Verthelyi, D. (2016). Zika (PRVABC59) Infection Is Associated with T cell Infiltration and Neurodegeneration in CNS of Immunocompetent Neonatal C57Bl/6 Mice. PLoS Pathog. *12*, e1006004.

Manangeeswaran, M., Kielczewski, J.L., Sen, H.N., Xu, B.C., Ireland, D.D.C., McWilliams, I.L., Chan, C.C., Caspi, R.R., and Verthelyi, D. (2018). ZIKA virus infection causes persistent chorioretinal lesions. Emerg. Microbes Infect. *7*, 96.

Marzi, A., Feldmann, F., Geisbert, T.W., Feldmann, H., and Safronetz, D. (2015a). Vesicular stomatitis virus-based vaccines against Lassa and Ebola viruses. Emerg. Infect. Dis. *21*, 305–307.

Marzi, A., Kercher, L., Marceau, J., York, A., Callsion, J., Gardner, D.J., Geisbert, T.W., and Feldmann, H. (2015b). Stat1-Deficient Mice Are Not an Appropriate Model for Efficacy Testing of Recombinant Vesicular Stomatitis Virus-Based Filovirus Vaccines. J. Infect. Dis. *212* (*Suppl 2*), S404–S409.

Marzi, A., Robertson, S.J., Haddock, E., Feldmann, F., Hanley, P.W., Scott, D.P., Strong, J.E., Kobinger, G., Best, S.M., and Feldmann, H. (2015c). EBOLA VACCINE. VSV-EBOV rapidly protects macaques against infection with the 2014/15 Ebola virus outbreak strain. Science *349*, 739–742.

Mattia, J.G., Vandy, M.J., Chang, J.C., Platt, D.E., Dierberg, K., Bausch, D.G., Brooks, T., Conteh, S., Crozier, I., Fowler, R.A., et al. (2016). Early clinical sequelae of Ebola virus disease in Sierra Leone: a cross-sectional study. Lancet Infect. Dis. *16*, 331–338.

Miner, J.J., and Diamond, M.S. (2016). Understanding How Zika Virus Enters and Infects Neural Target Cells. Cell Stem Cell *18*, 559–560.

Mire, C.E., Miller, A.D., Carville, A., Westmoreland, S.V., Geisbert, J.B., Mansfield, K.G., Feldmann, H., Hensley, L.E., and Geisbert, T.W. (2012). Recombinant vesicular stomatitis virus vaccine vectors expressing filovirus glycoproteins lack neurovirulence in nonhuman primates. PLoS Negl. Trop. Dis. *6*, e1567.

Pavot, V. (2016). Ebola virus vaccines: where do we stand? Clin. Immunol. *173*, 44–49.

Pedras-Vasconcelos, J.A., Goucher, D., Puig, M., Tonelli, L.H., Wang, V., Ito, S., and Verthelyi, D. (2006). CpG oligodeoxynucleotides protect newborn mice from a lethal challenge with the neurotropic Tacaribe arenavirus. J. Immunol. *176*, 4940–4949.

Rose, N.F., Roberts, A., Buonocore, L., and Rose, J.K. (2000). Glycoprotein exchange vectors based on vesicular stomatitis virus allow effective boosting and generation of neutralizing antibodies to a primary isolate of human immunodeficiency virus type 1. J. Virol. *74*, 10903–10910.

Sagui, E., Janvier, F., Baize, S., Foissaud, V., Koulibaly, F., Savini, H., Maugey, N., Aletti, M., Granier, H., and Carmoi, T. (2015). Severe Ebola Virus Infection With Encephalopathy: Evidence for Direct Virus Involvement. Clin. Infect. Dis. *61*, 1627–1628.

Scott, J.T., Sesay, F.R., Massaquoi, T.A., Idriss, B.R., Sahr, F., and Semple, M.G. (2016). Post-Ebola Syndrome, Sierra Leone. Emerg. Infect. Dis. *22*, 641–646.

Shirey, K.A., Pletneva, L.M., Puche, A.C., Keegan, A.D., Prince, G.A., Blanco, J.C., and Vogel, S.N. (2010). Control of RSV-induced lung injury by alternatively activated macrophages is IL-4R alpha-, TLR4-, and IFN-beta-dependent. Mucosal Immunol. *3*, 291–300.

Steptoe, P.J., Scott, J.T., Baxter, J.M., Parkes, C.K., Dwivedi, R., Czanner, G., Vandy, M.J., Momorie, F., Fornah, A.D., Komba, P., et al. (2017). Novel Retinal Lesion in Ebola Survivors, Sierra Leone, 2016. Emerg. Infect. Dis. *23*, 1102–1109.

Suder, E., Furuyama, W., Feldmann, H., Marzi, A., and de Wit, E. (2018). The vesicular stomatitis virus-based Ebola virus vaccine: From concept to clinical trials. Hum. Vaccin. Immunother. *14*, 2107–2113.

van den Pol, A.N., Mao, G., Chattopadhyay, A., Rose, J.K., and Davis, J.N. (2017a). Chikungunya, Influenza, Nipah, and Semliki Forest Chimeric Viruses with Vesicular Stomatitis Virus: Actions in the Brain. J. Virol. *91*, e02154-16.

van den Pol, A.N., Mao, G., Yang, Y., Ornaghi, S., and Davis, J.N. (2017b). Zika Virus Targeting in the Developing Brain. J. Neurosci. *37*, 2161–2175.

Varkey, J.B., Shantha, J.G., Crozier, I., Kraft, C.S., Lyon, G.M., Mehta, A.K., Kumar, G., Smith, J.R., Kainulainen, M.H., Whitmer, S., et al. (2015). Persistence of Ebola Virus in Ocular Fluid during Convalescence. N. Engl. J. Med. *372*, 2423–2427.

Vernon, P.S., and Griffin, D.E. (2005). Characterization of an in vitro model of alphavirus infection of immature and mature neurons. J. Virol. *79*, 3438–3447.

Wong, G., Mendoza, E.J., Plummer, F.A., Gao, G.F., Kobinger, G.P., and Qiu, X. (2018). From bench to almost bedside: the long road to a licensed Ebola virus vaccine. Expert Opin. Biol. Ther. *18*, 159–173.

World Health Organization (2000). Leishmania/HIV co-infection in South-western Europe 1990-1998: retrospective analysis of 965 cases.http://apps.who.int/iris/handle/10665/66625, WHO/LEISH/2000.42.

World Health Organization (2017). Meeting of the Strategic Advisory Group of Experts on immunization - conclusions and recommendations: Ebola vaccines, June 2017. https://www.who.int/csr/resources/publications/ebola/sage-vaccines-2017/en/.

World Health Organization (2018). Using vaccines in the fight against Ebola virus disease.https://www.who.int/immunization/policy/sage/news_vaccines_ebola_virus_disease/en/.

STAR★METHODS

KEY RESOURCES TABLE

REAGENT or RESOURCE	SOURCE	IDENTIFIER
Antibodies		
Rabbit anti-Ebola GP [Clone: KZ52]	Absolute Antibodies	Cat# Ab00690-23.0
Mouse anti-mouse neurofilament, heavy [Clone: SMI-31]	BioLegend	Cat# 801601; RRID:AB_2564641
Mouse anti-mouse neurofilament, heavy [Clone: SMI-32]	BioLegend	Cat# 801701; RRID:AB_2564642
Mouse anti-GAD67 [Clone: 1G10.2]	Millipore Sigma	Cat# MAB5406; RRID:AB_2278725
Chicken anti-GFAP polyclonal antibody	Novus Biologicals	Cat# NBP1-05198; RRID:AB_1556315
Mouse anti-NeuN [Clone: A60]	Millipore Sigma	Cat# MAB377; RRID:AB_2298772
Goat anti-rabbit IgG Secondary Ab Alexa Fluor 568	ThermoFisher	Cat# A11036; RRID:AB_10563566
Goat anti-rabbit IgG Secondary Ab Alexa Fluor Plus 647	ThermoFisher	Cat# A32733; RRID:AB_2633282
Goat anti-chicken IgY Secondary Ab Alexa Fluor 488	ThermoFisher	Cat# A11039; RRID:AB_2534096
Goat anti-chicken IgY Secondary Ab Alexa Fluor 568	ThermoFisher	Cat# A11041; RRID:AB_2534098
Goat anti-chicken IgY Secondary Ab Alexa Fluor 647	ThermoFisher	Cat# A21449; RRID:AB_2535866
Goat anti-mouse IgG Secondary Ab Alexa Fluor 488	ThermoFisher	Cat# A11017; RRID:AB_2534084
Goat anti-mouse IgG Secondary Ab Alexa Fluor 568	ThermoFisher	Cat# A11019; RRID:AB_143162
Mouse anti-mouse neurofilament-160 [Clone: NN18]	Sigma	Cat# N5264; RRID:AB_477278
Rat anti-mouse GFAP-eFluor 660 [Clone: GA5]	eBioscience	Cat# 50-9892-82; RRID:AB_2574408
Goat anti-mouse alexa fluor 488	Life Technologies	Cat# A11001; RRID:AB_2534069
Goat anti-rabbit alexa fluor 555	Life Technologies	Cat# A21428; RRID:AB_2535849
Bacterial and Virus Strains		
VSV (Indiana strain)	ATCC	VR-1238
rVSVΔG-ZEBOV-GP	BEI Resources	N/A
rVSVΔG-ZEBOV-GPΔMUC	Gift: Gerardo Kaplan (this paper)	N/A
rVSVΔG-RESTON-GP	Gift: Keith Peden (Lee et al., 2017)	N/A
Chemicals, Peptides, and Recombinant Proteins		
ProLong Diamond Antifade w/ DAPI	ThermoFisher	Cat# P36962
Fluoro-jade C Stain	EMD Millipore	Cat# AG32530MG
DAPI	ThermoFisher	Cat# D3571
DAPI	Thermo Scientific	Cat# 62248
DPX Mountant for histology	Sigma	Cat# 06522
Critical Commercial Assays		
TaqMan Fast Advanced Master Mix	ThermoFisher	Cat# 4444557
TURBO DNA-free Kit	ThermoFisher	Cat# AM1907
High-Capacity cDNA Reverse Transcription Kit	ThermoFisher	Cat# 4368813
ApopTag FITC *in situ* apoptosis detection kit	EMD Millipore	Cat# S7110
Experimental Models: Cell Lines		
VERO-E6	ATCC	CRL-1586; RRID:CVCL_0574
Experimental Models: Organisms/Strains		
Mouse: C57BL/6J	The Jackson Laboratory	Cat# 000664; RRID:IMSR_JAX:000664
Mouse: IFNAR1−/− (B6.129S2-Ifnar1tm1Agt/Mmjax)	The Jackson Laboratory	Cat# 032045-JAX; RRID:MMRRC_032045-JAX
Mouse: RAG1−/− (B6.129S7-Rag1tm1Mom/J)	The Jackson Laboratory	Cat# 002216; RRID:IMSR_JAX:002216
Mouse: MDA5−/− (B6.Cg-Ifih1tm1.1Cln/J)	The Jackson Laboratory	Cat# 015812; RRID:IMSR_JAX:015812
Mouse: IFNb−/−	Gift: Dr. Stefanie Vogel (Shirey et al., 2010)	N/A

(*Continued on next page*)

Continued

REAGENT or RESOURCE	SOURCE	IDENTIFIER
Oligonucleotides		
Cxcl10 mouse taqman primers	ThermoFisher	Cat# Mm00445235_m1
Gapdh mouse taqman primers	ThermoFisher	Cat# Mm99999915_g1
Ccl5 mouse taqman primers	ThermoFisher	Cat# Mm01302427_m1
Irf7 mouse taqman primers	ThermoFisher	Cat# Mm00516793_g1
Isg15 mouse taqman primers	ThermoFisher	Cat# Mm01705338_s1
Software and Algorithms		
Graphpad Prism v7.x	GraphPad software	N/A
Adobe Photoshop CC v20.x	Adobe	N/A
Adobe Illustrator CC v23.x	Adobe	N/A
Zeiss Zen v2	Zeiss	N/A
Olympus VS Software v2.9	Olympus	N/A
Quant-Studio Real-Time PCR System v1.2	Thermo Fisher Scientific	N/A
ImageJ with Fiji v1.50d	NIH	https://imagej.nih.gov/ij/

CONTACT FOR REAGENT AND RESOURCE SHARING

Further information and requests for resources and reagents should be directed to and will be fulfilled by the Lead Contact, Daniela Verthelyi (Daniela.Verthelyi@fda.hhs.gov).

EXPERIMENTAL MODEL AND SUBJECT DETAILS

Mice

C57BL/6J (B6), B6.IFNAR1$^{-/-}$, B6.MDA5$^{-/-}$, and B6.RAG1$^{-/-}$ mice were purchased from Jackson Laboratory. B6.IFNβ$^{-/-}$ mice were kindly provided by Dr. Stefanie Vogel at UMD (Shirey et al., 2010). Naive three-day-old (P3) neonatal mice, P7 neonatal mice, and 6-12-week-old adult mice born from specific pathogen-free parents were randomly split into groups for use in this study. In studies where mice inoculated at P3 or P7, animals were not separated by gender as gender assignment is difficult before day 15. In adults, studies in B6.IFNAR1$^{-/-}$ mice (6-12 week old) included male and female mice, and no gender-based difference was observed in the response to challenge. Inoculations of adult WT C57BL/6 mice were performed in 6-10 weeks old females. Mice were bred and housed in the FDA AAALAC accredited, pathogen-free animal facility. Mice were housed in standard cages with 1 breeding pair or up to 5 single sex mice per cage and a 12/12 light/dark schedule and fed on commercial 5P76 Prolab Isopro RMH 3000 diet. The experimental protocol was reviewed and approved by the FDA Animal Care and Use Committee (FDA-ACUC) and all animals used in these studies conform to relevant regulatory standards. All procedures were performed in accordance with the FDA ACUC guidelines.

Psuedotyped Viruses

We obtained VSV from ATCC and the VSV-G-deleted Vesicular Stomatitis Virus containing the Zaire (Mayinga) Ebolavirus GP (rVSVΔG-ZEBOV-GP) from BEI Resources (Established by NIAID and maintained by ATCC). The rVSVΔG-ZEBOV-GPΔMUC virus was a gift from Dr. Gerardo Kaplan. The rVSVΔG-RESTON-GP virus was a gift from Dr. Keith Peden (Lee et al., 2017). Viral stocks were passaged in Vero E6 cells to produce a master stock and stored at –80°C. Viral quantification of stocks was performed by $TCID_{50}$.

Cell lines

VERO E6 kidney epithelial cell-line was purchased from ATCC (Cat#CRL-1586) and cultured in MEM media containing 10% FBS, 1% Pen-Strep, and 1% L-Glutamine in a 37°C, 5% CO2 incubator for the duration of culture. The sex of this cell line is not specified by ATCC.

METHOD DETAILS

Mouse infections

Viral stocks were freshly thawed before each infection and diluted to working concentration to administer 1000 $TCID_{50}$ of virus in 50ul sterile phosphate buffer solution SC in the scruff of the neck of P3 neonatal mice and SC on the lower left quadrant of the abdomen of adult mice. WT VSV was administered at doses ranging from 10-1000 $TCID_{50}$ with similar outcome. Mice that were determined to be

moribund per criteria pre-established in the protocol by laboratory or animal staff were euthanized and counted as dead. Weight change was calculated as the change in the mean experimental group weight over time for each experiment [(Average group weight at day X post infection)/ (Average starting weight for the same group) * 100]. Mice that were euthanized to collect tissues for IHC were immediately exsanguinated by perfusion with cold PBS.

$TCID_{50}$ viral quantification

VERO E6 cells were plated in 100ul of complete MEM media in a 96 well plate to a target confluency of 70%–90% at 24 hours after plating. Organs were homogenized and cleared of cellular debris by centrifugation. The cleared supernatant was then serial diluted in non-supplemented MEM media and 100ul/well was plated in the VERO E6 96 well plate. Cytopathic effect was read 4-5 days after inoculation and $TCID_{50}$ was calculated as previously described (Manangeeswaran et al., 2016).

RNA extraction and q-PCR

Blood was collected by cardiac puncture into Trizol from infected animals 24-hour post infection and stored at −80°C until RNA was isolated (per Trizol manufacturers' protocol). RNA concentration and purity were determined by spectrophotometry at 260 nm and 280 nm using a NanoDrop 1000 spectrophotometer (ThermoFisher). After DNase treatment of 1 μg of RNA (DNA-free Turbo kit, ThermoFisher), reverse transcription was performed to generate cDNA using Multiscript High Capacity Reverse Transcriptase (ThermoFisher) using random primers per manufacturer's protocol. The cDNA was then diluted 5x with ultra-pure water and stored at −20°C. Gene quantification from cDNA was performed using a Viia7 real-time PCR machine with Quant Studio software. Gene fold change in expression (ΔΔCt) was determined by normalizing Ct values to GAPDH (housekeeping gene) and then to P3 non-infected, non-treated controls.

Eye histopathology and imaging

Mice inoculated with rVSVΔG-ZEBOV-GP or saline were sacrificed at 3, 6, or 9DPI to collect their eyes. Mice were perfused with sterile PBS before collection of eyes and placed into 4% PFA for 2 hours before being moved to cold sterile PBS. For histopathology, eyes were fixed for an additional 24hrs in formalin until they were embedded in methacrylate. The eyes were serially sectioned in the pupillary-optic nerve plane and then stained with hematoxylin and eosin (H&E). For immunocytochemistry, eyes were washed in PBS prior to cryopreservation in 20% sucrose and Tissue-Tek O.C.T. (Sakura-Finetek, Torrance, CA). The tissue blocks were stored at −80 degrees until cut into 12 μm sections and placed on SuperFrost Plus slides (Fisher Scientific, Carlsbad, CA). The slides were stored at −80◦C degrees until use. Frozen retinal sections thawed at room temperature, washed in PBS for 10 minutes, and then blocked with 10% normal goat serum and 0.03% Triton X-100 at room temperature for 1 h. The blocked tissue was washed with PBS for 10 minutes and stained with primary antibodies (1:50–1:200 dilution) overnight in blocking solution at 4°C in humid chambers to prevent the slides from drying out. The sections were then washed with PBS three times for 10 minutes. Staining involved rabbit anti-Ebola KZ52 (Absolute Antibody, 1:50), mouse anti-neurofilament-160 (Sigma; 1:100), and rat anti-GFAP directly conjugated to alexa fluor 633 (eBioScience, 1:100) along with DAPI (Invitrogen; 1:500 dilution) at room temperature. Goat anti-mouse alexa fluor 488 and goat anti-rabbit alexa fluor 555 (Molecular Probes; 1:500 dilution) were used as secondary antibodies. The slides were then washed three times in PBS and mounted with ProLong Gold (Molecular Probes).

Brain immunohistochemistry and confocal imaging

Infected mice were euthanized at 3, 6, and 9 days post infection and perfused with sterile, 1 x PBS (GIBCO). One hemisphere of the brain from each mouse was collected and immediately placed 4% paraformaldehyde for 24 hours before being transferred into 30% (w/v) sucrose solution until the brains were fully infused with sucrose. Brains were then embedded in TissueTek O.C.T (Sakura-Finetek, Torrance, CA) mounting media and 30 μm sections cut using a Leica CM1900 cytostat (Leica Biosystems, Buffalo Grove, IL), mounted onto superfrost plus microscope slides (Fisher Scientific) and stored at −80◦C. For immunofluorescence-immunohistochemistry (IF-IHC), slides were warmed and allowed to dry at room temperature. The sections were then hydrated in 1 x PBS (GIBCO), followed by antigen retrieval in sodium citrate buffer, pH 9.0 at 80°C for 8 minutes and 10 minutes of cooling. The sections were then permeabilized in Triton X-100 for 1 hour at RT. TUNEL staining was performed after antigen retrieval as per manufacturers' instructions (EMD Millipore ApopTag-FITC kit), followed by IF-IHC co-staining. For IF-IHC, sections were incubated for at least 1 hour at RT in 5% normal goat serum, diluted in 1% bovine serum albumin and 0.05% Triton X-100 in 1 x PBS to block non-specific binding. The sections were then stained with combinations of anti-NeuN (EMD Millipore), anti-GFAP (ProteinTech group), anti-Neurofilament heavy chain (NF-H) cocktail (anti-NF-H clone SMI-31 and anti-NF-H clone SMI-31 combined, BioLegend), anti-GAD67 (EMD Millipore) and Rabbit-anti-Ebola GP (KZ52). Primary antibodies were diluted in dilution buffer (1% BSA + 0.05% Triton X-100 in PBS) and applied for 24 hours at RT. Sections were then incubated with species appropriate highly cross-absorbed Alexa Fluor conjugated (ThermoFisher) goa- anti-IgG secondary antibodies in dilution buffer for at least 2 hours at RT. All slides were then mounted with Prolong Diamond Anti-Fade mounting media containing DAPI (ThermoFisher, Carlsbad, CA). Whole section images were acquired using an Olympus VS-120 Virtual Microscope, using Olympus VS software (Olympus LSS). Fluoro-Jade C staining was performed as per the manufacturers protocol (EMD Millipore, Billerica, MA). Regions of interest noted in acquired sections were imaged using a Zeiss LSM 880 confocal microscope equipped with a 405 nm, 488 nm, 561 nm and 633 nm lasers. For each stain, optimal laser and PMT settings were determined using control sections and then applied for similarly stained tissues. Zeiss Zen software was

used to acquire images. Multiple Z-planes were imaged in each region, with optimal spacing determined for each objective lens. Images shown are maximum intensity projections of acquired Z-planes.

QUANTIFICATION AND STATISTICAL ANALYSIS

Analysis of gene induction between naive mice treated with Poly (I:C) was performed using an unpaired two-tailed t test, and data is shown as mean ± standard deviation (SD). Analysis of gene induction between infected mice co-treated with Poly (I:C) was tested using one-way ANOVA with post hoc Tukey's multiple comparison test, and data is shown as mean ± SD. The experimental replicates and value of "n," which represents the number of mice included in each study, is stated in each corresponding figure. Statistical significance is indicated as "ns" for not significant; * for $p < 0.05$; ** for $p < 0.01$; *** for $p < 0.001$. All analyses were carried out in GraphPad Prism.